1492 Bull. Chem. Soc. Jpn. Vol. 81, No. 11, 1492–1499 (2008)

Charge-Transfer Complexes between Indoline–Tricyanoquinodimethane Compounds and 7,7,8,8-Tetracyanoquinodimethane

Tsuyoshi Murata,*[1] Genki Honda,[1] Chin-Hong Chong,[1] Masaru Makihara,[1] Kazukuni Nishimura,[1] Salavat Khasanov,[1,2] Akihiro Otsuka,[3] and Gunzi Saito*[1,3,4]

[1]Division of Chemistry, Graduate School of Science, Kyoto University, Sakyo-ku, Kyoto 606-8502

[2]The Institute of Solid State Physics of Russian Academy of Science, Chernogolovka 142432, Russia

[3]Research Center for Low Temperature and Materials Sciences, Kyoto University, Sakyo-ku, Kyoto 606-8502

[4]Research Institute, Meijo University, Tenpaku-ku, Nagoya 468-8502

Received March 19, 2008; E-mail: saito@kuchem.kyoto-u.ac.jp, tmurata@kuchem.kyoto-u.ac.jp

Intramolecular charge-transfer compounds composed of 1-alkyl-3,3-dimethyl-2-methyleneindoline ($\mathbf{I}_n$, donor, n = alkyl chain length; 1 or 6) and 7,8,8-tricyanoquinodimethane (=2-(4′-cyanomethylene-2′,5′-cyclohexadienylidene)-malononitrile, 3CNQ, acceptor) moieties afforded charge-transfer complexes with 7,7,8,8-tetracyanoquinodimethane (TCNQ): ($\mathbf{I}_1$–3CNQ)$_2$(TCNQ) and ($\mathbf{I}_6$–3CNQ)(TCNQ). ($\mathbf{I}_1$–3CNQ)$_2$(TCNQ) included two kinds of $\mathbf{I}_1$–3CNQ molecules of different molecular conformations. ($\mathbf{I}_1$–3CNQ)$_2$(TCNQ) and ($\mathbf{I}_6$–3CNQ)(TCNQ) were constructed from one-dimensional columns of 3CNQ···TCNQ···3CNQ triads and 3CNQ···TCNQ dyads, respectively. These complexes exhibited intermolecular charge-transfer bands extending to the near IR region (1000–1500 nm) in addition to intramolecular charge-transfer bands around 600–900 nm characteristic of $\mathbf{I}_n$–3CNQ compounds. They were characterized as weak charge-transfer solids from estimations of the degree of charge transfer using molecular orbital calculations, bond lengths, and vibration spectra. Intermolecular charge transfer caused a slight increase in the degree of intramolecular charge transfer.

Unimolecular donor (D) and acceptor (A) compounds linked by a π-bond ($\mathrm{D}^{\delta+}$–π–$\mathrm{A}^{\delta-}$, δ = degree of intramolecular charge transfer (CT)) exhibit flexible electronic structures and large dipole moments originating from intramolecular CT processes. Such features of $\mathrm{D}^{\delta+}$–π–$\mathrm{A}^{\delta-}$ are significant as potential sources for organic optical materials, such as non-linear optics,[1–11] photovoltaics,[12] and photochromics.[1,13] In addition to intramolecular CT phenomena, $\mathrm{D}^{\delta+}$–π–$\mathrm{A}^{\delta-}$ compounds show amphoteric redox abilities, and have been widely utilized in research of unimolecular rectifiers[14–18] and organic semiconductors.[19] Besides such intramolecular CT compounds, binary CT complexes composed of D and A molecules have also provided numerous intriguing materials, such as organic (super)conductors,[20–24] magnetic materials,[25] and unusual phase-transition systems (neutral–ionic transition[26,27] and photo-induced phase transition[28]); however, CT complexes of unimolecular $\mathrm{D}^{\delta+}$–π–$\mathrm{A}^{\delta-}$ compounds have not been reported previously to our best knowledge.[29]

We have recently been studying syntheses, crystal structures, and optical properties of indoline (**I**)–tricyanoquinodimethane (=2-(4′-cyanomethylene-2′,5′-cyclohexadienylidene)-malononitrile, 3CNQ) $\mathrm{D}^{\delta+}$–π–$\mathrm{A}^{\delta-}$ compounds ($\mathbf{I}_n$–3CNQ-R, n = alkyl chain length and R = substituent group on the 3CNQ moiety, Chart 1).[30–32] Our studies demonstrated that the δ values of $\mathbf{I}_n$–3CNQ-R are tunable by chemical modifications and significantly affect the molecular (hyper)polarizabilities and non-linear optical properties.[32] Furthermore, we revealed that the δ values are sensitive to environmental perturbations such as molecular conformation, molecular packing, and solvent polarity.[31,32] In the study of $\mathrm{D}^{\delta+}$–π–$\mathrm{A}^{\delta-}$ compounds, we obtained CT complexes between $\mathbf{I}_n$–3CNQ compounds and TCNQ. In the present study, we present the crystal structures, estimations of degrees of intra- and intermolecular CT, and optical properties of ($\mathbf{I}_1$–3CNQ)$_2$(TCNQ) and ($\mathbf{I}_6$–3CNQ)(TCNQ). The effect of intermolecular CT on the degrees of intramolecular CT of $\mathbf{I}_n$–3CNQ molecules was also discussed.

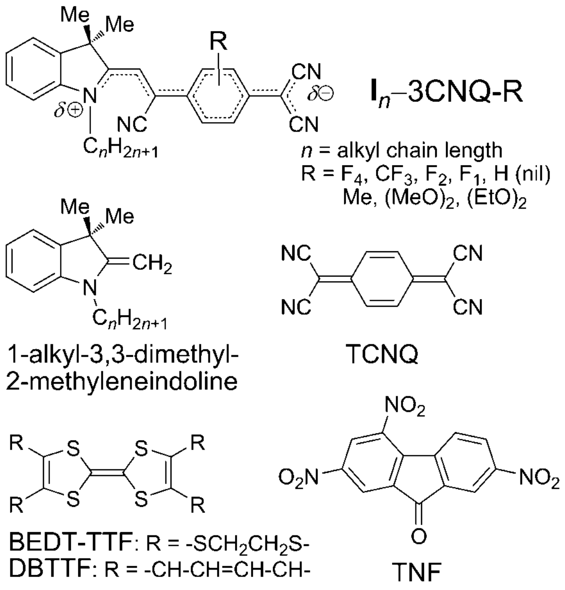

Chart 1. Chemicals discussed in this study.

Published on the web November 12, 2008; doi:10.1246/bcsj.81.1492

Experimental

Materials. $\mathbf{I}_1$–3CNQ and $\mathbf{I}_6$–3CNQ were prepared according to our previous papers.[30,31] TCNQ was purified by sublimation.

Measurements. Melting points were measured with a Yanaco MP-500D micro melting-point apparatus and were not corrected. Elemental analyses were performed at the Center for Organic Elemental Microanalysis, Kyoto University. Ultraviolet–visible (UV–vis) spectra were measured on a Shimadzu UV-3100 spectrometer in acetonitrile (MeCN) solutions or KBr pellets. IR spectra of the samples in KBr pellet were measured using a Perkin-Elmer PARAGON 1000 FT-IR spectrometer (resolution $4\,\text{cm}^{-1}$).

Preparation of ($\mathbf{I}_1$–3CNQ)$_2$(TCNQ). Hot solutions of $\mathbf{I}_1$–3CNQ (70.0 mg, 0.20 mmol) in MeCN (30 mL) and TCNQ (20.4 mg, 0.10 mmol) in MeCN (20 mL) were mixed, and then cooled to room temperature. The resulting crystals were collected by filtration, to yield the complex (45.0 mg, 50%) as dark reddish purple plate crystals. Mp 230–232 °C (dec); Anal. Calcd for $(C_{23}H_{18}N_4)_2(C_{12}H_4N_4)$: C, 76.97; H, 4.45; N, 18.57%. Found: C, 77.02; H, 4.68; N, 18.61%.

Preparation of ($\mathbf{I}_6$–3CNQ)(TCNQ). Hot solutions of $\mathbf{I}_6$–3CNQ (89.8 mg, 0.21 mmol) in MeCN (30 mL) and TCNQ (21.4 mg, 0.11 mmol) in MeCN (20 mL) were mixed. The resulting mixture was slowly concentrated under atmosphere, to yield the complex (36.3 mg, 53%) as reddish purple plate crystals. Mp 201–203 °C (dec); Anal. Calcd for $(C_{28}H_{28}N_4)(C_{12}H_4N_4)$; C, 76.90; H, 5.16; N, 17.94%. Found: C, 77.00; H, 5.16; N, 17.96%. The product included un-reacted $\mathbf{I}_6$–3CNQ (yellow green blocks), and the complex was separated by hand.

X-ray Crystal Structure Analyses. The intensity data of structural analyses were collected using a Bruker AXS DIP-2020K oscillator type X-ray imaging plate with monochromated Mo Kα ($\lambda = 0.71073$ Å, 1 Å = 0.1 nm) radiation. Structures were determined by a direct method using SHELXS-97.[33] Refinements were performed by the full-matrix least-squares method on F^2 with SHELXL-97.[34] All non-hydrogen atoms were refined anisotropically. Hydrogen atoms were included without refinement. Positions of the hydrogen atoms were calculated assuming sp^3 or sp^2 conformations of carbon atoms. Crystallographic parameters are summarized in Table 1. Crystallographic data have been deposited with Cambridge Crystallographic Data Centre: Deposition numbers CCDC-232865 and 693070. Copies of the data can be obtained free of charge via http://www.ccdc.cam.ac.uk/conts/retrieving.html (or from the Cambridge Crystallographic Data Centre, 12, Union Road, Cambridge, CB2 1EZ, UK; Fax: +44 1223 336033; e-mail: deposit@ccdc.cam.ac.uk).

Calculation. Intermolecular overlaps were calculated based on the crystal structures by the extended Hückel method with single ζ parameters. Semi-empirical molecular orbital (MO) calculations were performed using MOS/F V4 with INDO/S parameterization coupled with a 20-dimensional CI matrix, which is sufficient to obtain approximately invariant atomic charge. Geometrical parameters were extracted from the crystal structures.

Results and Discussion

Preparation. $\mathbf{I}_1$–3CNQ and $\mathbf{I}_6$–3CNQ exhibit amphoteric redox behaviors with irreversible processes in cyclic voltammetry (CV), and their redox abilities are very close to each other ($E_\text{p}^\text{red} = -0.45$ V and $E_\text{p}^\text{ox} = +0.57$ V for $\mathbf{I}_1$–3CNQ; $E_\text{p}^\text{red} = -0.41$ V and $E_\text{p}^\text{ox} = +0.60$ V for $\mathbf{I}_6$–3CNQ, V vs. SCE).[31] Their electron-accepting abilities are much weaker than that of TCNQ ($E_{1/2}^\text{red} = +0.22$ V) and similar to that of 2,4,7-trinitrofluorenone (TNF, Chart 1, $E_{1/2}^\text{red} = -0.43$ V). Electron-donating abilities of $\mathbf{I}_1$–3CNQ and $\mathbf{I}_6$–3CNQ are slightly weaker than that of BEDT-TTF ($E_{1/2}^\text{ox} = +0.53$ V) and slightly stronger than that of DBTTF ($E_{1/2}^\text{ox} = +0.62$ V). DBTTF is known to give a CT complex having a neutral ground state with TCNQ,[35] and BEDT-TTF affords both neutral and mixed-valent CT complexes with TCNQ depending on the reaction conditions.[36] Mixing of a solution of $\mathbf{I}_1$–3CNQ or $\mathbf{I}_6$–3CNQ with that of TCNQ in MeCN yielded reddish purple crystals, which are characterized as 2:1 and 1:1 complexes, respectively, by elemental analyses. Both complexes are insulators (room temperature conductivity $<10^{-8}$ S cm^{-1}).

Table 1. Crystallographic Data of ($\mathbf{I}_1$–3CNQ)$_2$(TCNQ) and ($\mathbf{I}_6$–3CNQ)(TCNQ)

	($\mathbf{I}_1$–3CNQ)$_2$(TCNQ)	($\mathbf{I}_6$–3CNQ)(TCNQ)
Formula	$C_{58}H_{40}N_{12}$	$C_{40}H_{32}N_8$
F_w	905.02	624.74
Crystal habit	reddish purple plate	reddish purple plate
Crystal system	triclinic	triclinic
Space group	$P\bar{1}$	$P\bar{1}$
a/Å	8.0500(6)	9.086(1)
b/Å	15.621(2)	13.545(2)
c/Å	20.489(2)	15.155(2)
α/°	70.920(5)	102.806(7)
β/°	81.897(5)	97.481(8)
γ/°	87.003(6)	109.230(8)
V/Å^3	2410.6(4)	1674.9(4)
Z	2	2
d_calcd/g cm^{-1}	1.247	1.239
Temperature	RT	RT
μ (Mo Kα)/mm^{-1}	0.077	0.076
Unique reflections	8026	6231
No. of reflections	6236	3251
No. of parameters	677	409
R_1 ($I > 2.0\sigma(I)$)	0.046	0.083
$_wR_2$	0.121	0.239
GOF	1.021	1.066

Crystal Structures. **(A) Crystal Structure of ($\mathbf{I}_1$–3CNQ)$_2$(TCNQ):** This complex crystallized in a triclinic system, where two $\mathbf{I}_1$–3CNQ ($\mathbf{I}_1$–3CNQ-A and $\mathbf{I}_1$–3CNQ-B) and two halves of TCNQ (TCNQ-A and TCNQ-B) molecules having inversion centers are crystallographically independent. As shown in Figures 1a and 1b, $\mathbf{I}_1$–3CNQ-A and $\mathbf{I}_1$–3CNQ-B have different molecular conformations, where the *N*-alkyl group of indoline moiety is located close to (Type I) or far from (Type II) the CN group of 3CNQ moiety, respectively.

In the crystal structure, 3CNQ moieties of $\mathbf{I}_1$–3CNQ-A and $\mathbf{I}_1$–3CNQ-B molecules stack with TCNQ-A and TCNQ-B molecules, respectively, to form 3CNQ···TCNQ···3CNQ triads (triad-A and triad-B, respectively, Figure 1c). The triads stack with twisting by 21.7° along the c axis to form a one-dimensional column (Figure 1d). Effective intermolecular overlap integrals are observed only along the stacking direction, where those within triad-A and triad-B are similar to each other (16.1×10^{-3} and 17.0×10^{-3}, respectively) and larger than that between the triads (-3.6×10^{-3}). The indoline moieties

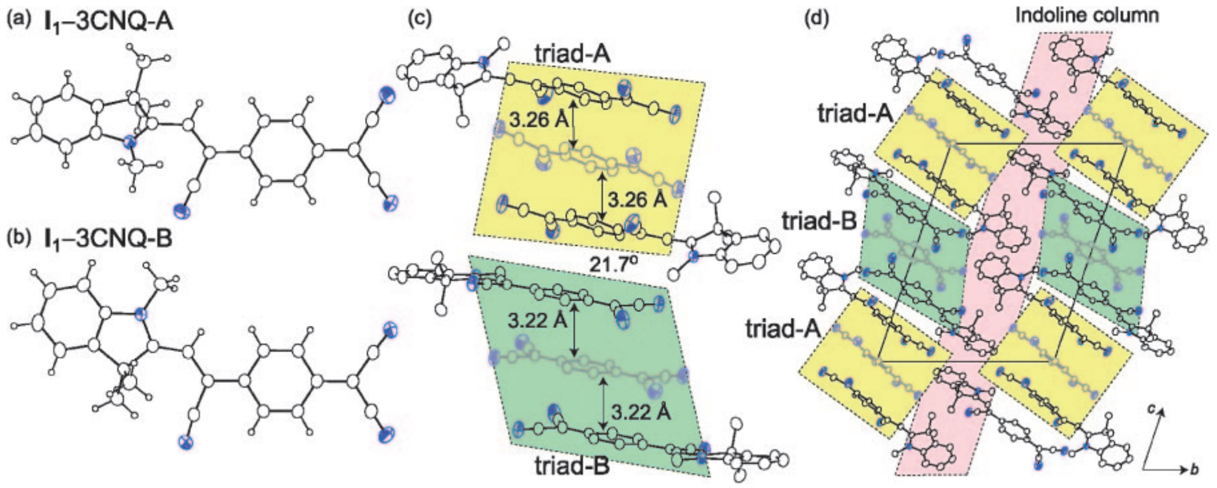

Figure 1. (a & b) Molecular structures of $\mathbf{I}_1$–3CNQ-A and $\mathbf{I}_1$–3CNQ-B, respectively. (c) One-dimensional column comprised of 3CNQ···TCNQ···3CNQ triads. (d) Molecular packing viewed along the *a* axis. TCNQ molecules are drawn in thin colors. Yellow and green areas show 3CNQ···TCNQ···3CNQ triads of $\mathbf{I}_1$–3CNQ-A and $\mathbf{I}_1$–3CNQ-B, respectively, and red area represents the assembly of indoline moieties. Hydrogen atoms are omitted in (c) and (d).

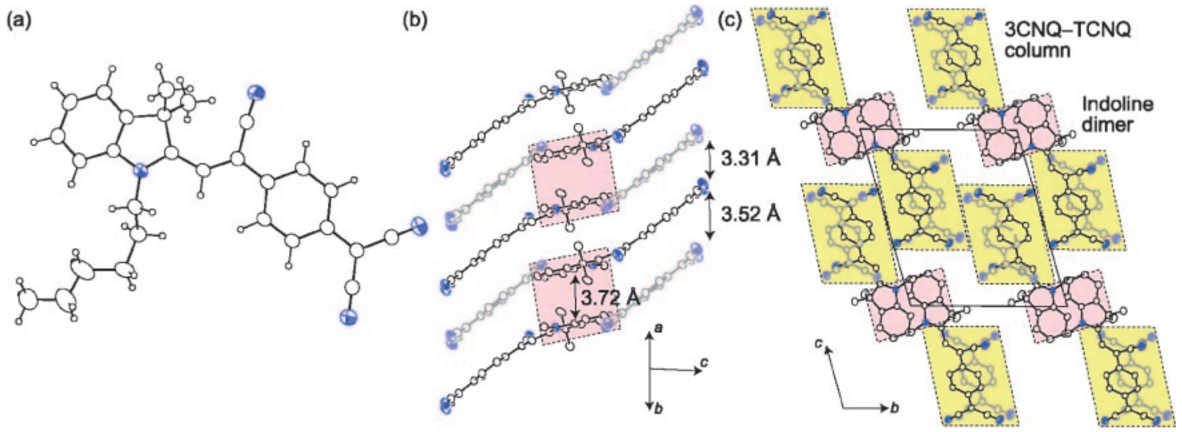

Figure 2. (a) Molecular structure of $\mathbf{I}_6$–3CNQ. (b) One-dimensional column composed of 3CNQ···TCNQ dyads. (c) Molecular packing viewed along the *a* axis. TCNQ molecules are drawn in thin colors. Yellow and red areas show 3CNQ···TCNQ columns and indoline dimers, respectively. Hydrogen atoms and hexyl groups are omitted in (b) and (c).

of $\mathbf{I}_1$–3CNQ-A and $\mathbf{I}_1$–3CNQ-B molecules individually stack with interplanar distances of 3.49 and 3.82 Å, respectively, to form dimers, and the dimers assemble along the *c* axis to form a columnar structure (Figure 1d).

(B) Crystal Structure of ($\mathbf{I}_6$–3CNQ)(TCNQ): This complex crystallized in a triclinic system, where one $\mathbf{I}_6$–3CNQ and one TCNQ molecule are crystallographically independent. The $\mathbf{I}_6$–3CNQ molecule has Type II molecular conformation (Figure 2a), which corresponds to those in the crystal structures of $\mathbf{I}_6$–3CNQ itself.[31]

The 3CNQ moieties stack with TCNQ molecules to form a one-dimensional alternating column (Figure 2b). The interplanar distances of the stacks are 3.31 and 3.52 Å, and the column composed of 3CNQ···TCNQ dyads. The overlap integral within the dyad is 28.6×10^{-3} and larger than that between neighboring dyads (1.0×10^{-3}). These columns are arranged along the *b* axis to establish a layered motif (Figure 2c). The indoline moiety also stacks with an interplanar distance of 3.72 Å to form a dimer motif (Figure 2b), and the dimers are separated by an alkyl chain.

Estimation of Degrees of Inter- and Intramolecular CT. In ($\mathbf{I}_1$–3CNQ)$_2$(TCNQ) and ($\mathbf{I}_6$–3CNQ)(TCNQ) complexes, the majority of intermolecular CT interactions occur between the 3CNQ moiety and the TCNQ molecule within the one-dimensional columns, since significant overlap integrals are observed only within these columns. Therefore, CT processes in the complexes are presented as Scheme 1, where the degree of intramolecular CT between indoline and 3CNQ moieties is δ, and that of intermolecular CT from 3CNQ moiety to TCNQ is ζ. Indoline and 3CNQ moieties have charges of $+\delta$ and $-(\delta - \zeta)$, respectively. Since ($\mathbf{I}_1$–3CNQ)$_2$(TCNQ) complex has a 2:1 ratio, its TCNQ molecule has a minus charge of -2ζ.

(A) Molecular Orbital Calculation: The degrees of CT of $D^{\delta+}$–π–$A^{\delta-}$ compounds and CT complexes express the charges on donor and acceptor moieties. We performed an MO calculation to investigate the degrees of CT. The summation of atomic charges on each moiety gives the degrees of CT: indoline ($+\delta_{\text{charge}}$), 3CNQ ($-(\delta_{\text{charge}} - \zeta_{\text{charge}})$), and TCNQ ($-X\zeta_{\text{charge}}$) moieties. In the crystal structures, significant overlap integrals are observed only in the 3CNQ···TCNQ···3CNQ

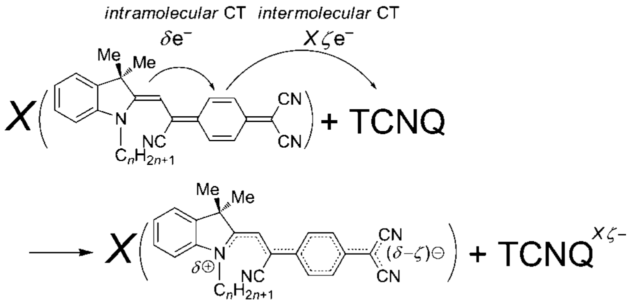

Scheme 1. Schematic presentation of CT processes in $(\mathbf{I}_n\text{–3CNQ})_X(\text{TCNQ})$ complexes. X shows the component ratio.

triad for $(\mathbf{I}_1\text{–3CNQ})_2(\text{TCNQ})$ and the 3CNQ···TCNQ dyad for $(\mathbf{I}_6\text{–3CNQ})(\text{TCNQ})$; therefore, the MO calculations were performed for the isolated pairs extracted from the crystal structures. Considering the values of atomic charges, the boundary between D and A parts of an $\mathbf{I}_n$–3CNQ is assumed to be located between indoline and cyanoethylene moieties (Table 2). The obtained CT degrees are summarized in Table 2 together with those for $\mathbf{I}_6$–3CNQ crystals.[31]

In the $(\mathbf{I}_1\text{–3CNQ})_2(\text{TCNQ})$ complex, the δ_{charge} value of $\mathbf{I}_1$–3CNQ-A (+0.65, Type I conformation, Figure 1a) is larger than that of $\mathbf{I}_1$–3CNQ-B (+0.51, Type II conformation, Figure 1b). This result corresponds to our previous study, where an $\mathbf{I}_n$–3CNQ molecule of Type I conformation has a larger δ value.[31] Compared with the difference in the δ_{charge} values between triad-A and triad-B, the difference in charges on TCNQ-A and TCNQ-B moieties ($-2\zeta_{\text{charge}} = -0.19$ and -0.16, respectively) is small, indicating that the effect of molecular conformations of $\mathbf{I}_1$–3CNQ molecules on the intermolecular CT is small. The δ_{charge} value of the $\mathbf{I}_6$–3CNQ molecule (+0.47) in the complex is larger by 0.07–0.10 than those in $\mathbf{I}_6$–3CNQ crystals (0.37–0.40). Similarly, the charge on the 3CNQ moiety ($-(\delta_{\text{charge}} - \zeta_{\text{charge}})$) in the $(\mathbf{I}_6\text{–3CNQ})(\text{TCNQ})$ complex is larger than those in $\mathbf{I}_6$–3CNQ crystals, although the difference is small compared with that in the δ_{charge} values. These results indicate that the intermolecular CT between the 3CNQ moiety and TCNQ molecule increases the δ value. Larger amounts of charges on TCNQ moieties in $(\mathbf{I}_1\text{–3CNQ})_2(\text{TCNQ})$ ($-2\zeta_{\text{charge}} = -0.19$ and -0.16) than that in $(\mathbf{I}_6\text{–3CNQ})(\text{TCNQ})$ ($-\zeta_{\text{charge}} = -0.05$) well reflect the component ratios.

Table 2. Charges of Indoline, 3CNQ, and TCNQ Moieties Obtained by the MO Calculation

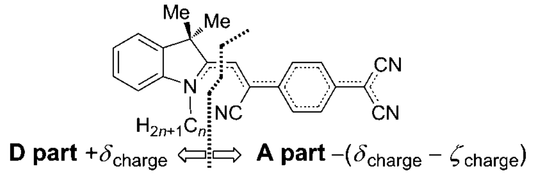

		Indoline	3CNQ	TCNQ
		(δ_{charge})	$(-(\delta_{\text{charge}} - \zeta_{\text{charge}}))$	$(-X\zeta_{\text{charge}})$
$(\mathbf{I}_1\text{–3CNQ})_2(\text{TCNQ})$[a)]	A	+0.65	−0.56	−0.19
	B	+0.51	−0.43	−0.16
$(\mathbf{I}_6\text{–3CNQ})(\text{TCNQ})$		+0.47	−0.42	−0.05
		+0.38	−0.38	—
$\mathbf{I}_6$–3CNQ[b) 31]		+0.37	−0.37	—
		+0.40	−0.40	—

a) Calculated for a $(\mathbf{I}_1\text{–3CNQ})_2(\text{TCNQ})$ triad. Calculated values for two $\mathbf{I}_1$–3CNQ molecules in each triad are very close to each other within the differences of 0.001. b) Three kinds of polymorphs have been found, where all $\mathbf{I}_6$–3CNQ molecules have a Type II conformation.

(B) Bond Length Ratio (*BLR*): It is well known that bond lengths (***a***–***c*** in Table 3) of TCNQ molecules exhibit bond alternation between neutral and radical anion states. The ratio of single and double bond lengths defined as $r = \boldsymbol{b}/(\boldsymbol{a} + \boldsymbol{c})$ shows a good linear relationship with the degree of CT (ζ), and has been utilized in the estimation of charges on TCNQ molecules in CT complexes.[37] Table 3 summarizes the bond lengths ***a***–***c*** and the estimated charges on TCNQ ($-X\zeta_{BLR}$) in $(\mathbf{I}_1\text{–3CNQ})_2(\text{TCNQ})$ and $(\mathbf{I}_6\text{–3CNQ})(\text{TCNQ})$. The charges on TCNQ molecules are relatively small; $-2\zeta_{BLR} = -0.21$ and -0.25 for TCNQ-A and TCNQ-B molecules, respectively, in $(\mathbf{I}_1\text{–3CNQ})_2(\text{TCNQ})$ and $-\zeta_{BLR} = 0.00$ for $(\mathbf{I}_6\text{–3CNQ})$-(TCNQ), indicating the neutral ground states ($-0.5 < -X\zeta \leq 0$) of these CT complexes. The smaller charge on the TCNQ molecule of $(\mathbf{I}_6\text{–3CNQ})(\text{TCNQ})$ than those of $(\mathbf{I}_1\text{–3CNQ})_2(\text{TCNQ})$ coincides with that obtained by the MO calculation.

In a previous study, we demonstrated that C–N and C–C bond lengths defined as $\boldsymbol{a}'$–$\boldsymbol{e}'$ exhibit a bond alternation between neutral and ionic forms (Scheme 2), and that the bond length ratio (*BLR*) value defined as $BLR = (\boldsymbol{b}' + \boldsymbol{d}' + \boldsymbol{e}')/(\boldsymbol{a}' + \boldsymbol{c}')$ shows a good linear relationship with the degree of intramolecular CT (δ) for $\mathbf{I}_n$–3CNQ-R molecules.[31] Since the

Table 3. Intramolecular Bond Lengths (***a***–***c***),[a)] r, and Charges on TCNQ Molecules in the CT Complexes

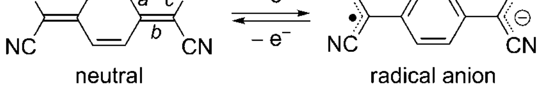

		a/Å	***b***/Å	***c***/Å	r[b)]	Charge ($-X\zeta_{BLR}$)[c)]
$(\mathbf{I}_1\text{–3CNQ})_2(\text{TCNQ})$	A	1.440(2)	1.385(2)	1.440(3)	0.4810(9)	−0.21
	B	1.437(3)	1.382(3)	1.428(3)	0.482(1)	−0.25
$(\mathbf{I}_6\text{–3CNQ})(\text{TCNQ})$		1.435(2)	1.373(3)	1.449(2)	0.476(1)	0.00
TCNQ^0[d)]		1.448(4)	1.374(3)	1.441(3)	0.476(1)	0.00
$\text{Rb}^+\text{TCNQ}^{\bullet-}$[d)]		1.423(4)	1.420(4)	1.416(4)	0.500(2)	−1.00

a) Å (1 Å = 0.1 nm). b) $r = \boldsymbol{b}/(\boldsymbol{a} + \boldsymbol{c})$. c) $-X\zeta_{BLR} = (r - r^0)/(r^1 - r^0)$, where r^0 and r^1 are the r values of TCNQ^0 and $\text{Rb}^+\text{TCNQ}^{\bullet-}$. d) See, Ref. 37.

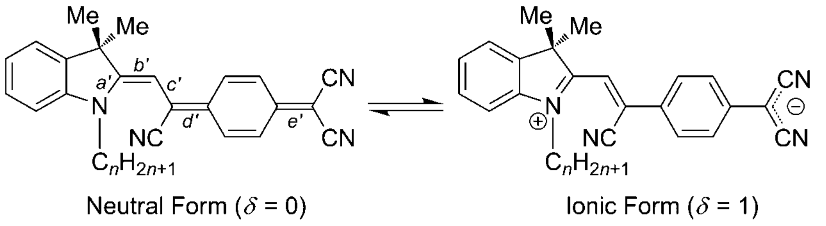

Scheme 2. Bond alternation of $\mathbf{I}_n$–3CNQ in neutral and ionic forms. ***a′*–*e′*** show the bond lengths sensitive to the δ value.

Table 4. Intramolecular Bond Lengths (***a′*–*e′***)[a] and *r′* of the 3CNQ Moieties in the CT Complexes

		a′/Å	***b′***/Å	***c′***/Å	***d′***/Å	***e′***/Å	*r′*[c]
($\mathbf{I}_1$–3CNQ)$_2$(TCNQ)	**A**	1.322(2)	1.427(2)	1.368(2)	1.439(2)	1.419(2)	2.089(4)
	B	1.342(2)	1.411(2)	1.383(2)	1.444(2)	1.415(2)	2.067(4)
($\mathbf{I}_6$–3CNQ)(TCNQ)		1.353(4)	1.411(5)	1.381(5)	1.436(5)	1.420(5)	2.068(8)
$\mathbf{I}_6$–3CNQ[b) 31]		1.347(3)	1.397(3)	1.398(3)	1.427(3)	1.408(3)	2.028(5)
		1.355(4)	1.389(4)	1.394(4)	1.431(4)	1.407(5)	2.036(6)
		1.351(3)	1.403(3)	1.388(3)	1.435(3)	1.417(3)	2.055(5)

a) Å (1 Å = 0.1 nm). b) Three kinds of polymorphs have been found, where all $\mathbf{I}_6$–3CNQ molecules have the Type II conformation. c) $r' = (\boldsymbol{d}' + \boldsymbol{e}')/\boldsymbol{c}'$.

charges on indoline (δ) and 3CNQ ($-(\delta - \zeta)$) moieties are different, the estimations of the degrees of CT should be performed individually for each moiety. We used the bond length ***a′*** and *BLR* defined as $r' = (\boldsymbol{d}' + \boldsymbol{e}')/\boldsymbol{c}'$ to discuss the charges on indoline and 3CNQ moieties, respectively (Table 4). Since $\delta = 0$ and 1 limits for the $\mathbf{I}_n$–3CNQ compounds have not been obtained at present, quantitative estimation of the δ values cannot be obtained from the *BLR* values.

In the ($\mathbf{I}_1$–3CNQ)$_2$(TCNQ) complex, the $\mathbf{I}_1$–3CNQ-A molecule has a shorter ***a′*** bond and a larger *r′* value than those of $\mathbf{I}_1$–3CNQ-B. This result indicates that the $\mathbf{I}_1$–3CNQ-A molecule of a Type I conformation has larger δ and $-(\delta - \zeta)$ values than those of $\mathbf{I}_1$–3CNQ-B of a Type II conformation, which is consistent with our previous study[31] and the MO calculation (Table 2). In the case of the $\mathbf{I}_6$–3CNQ molecule, a notable difference in the bond length ***a′*** is not found between molecules in the complex and $\mathbf{I}_6$–3CNQ crystals; however, the *r′* value of the complex is larger than those of $\mathbf{I}_6$–3CNQ crystals to some extent, implying that the $-(\delta - \zeta)$ value is increased by complex formation.

(C) IR Spectra: In the solid-state IR spectra, complexes ($\mathbf{I}_1$–3CNQ)$_2$(TCNQ) and ($\mathbf{I}_6$–3CNQ)(TCNQ) exhibit single C≡N stretching modes at around 2210–2220 cm^{-1} and multiple bands at around 2150–2200 cm^{-1} (Figure 3). Table 5 summarizes the C≡N stretching frequencies of the complexes together with those of related compounds.

The $\nu_{\text{C≡N}}$ (b_{1u}) mode of TCNQ in CT solids softens linearly with the degree of CT (0–0.5), and has been utilized in the estimation of the degree of CT: $X\zeta_{\text{C≡N}} = (\nu_0 - \nu_{\text{C≡N}})/(\nu_0 - \nu_1)$, where ν_0 and ν_1 are the $\nu_{\text{C≡N}}$ values of neutral (2227 cm^{-1}) and radical anion species (2183 cm^{-1}).[38] Such modes of ($\mathbf{I}_1$–3CNQ)$_2$(TCNQ) and ($\mathbf{I}_6$–3CNQ)(TCNQ) are observed at 2212 and 2216 cm^{-1}, respectively, and exhibit low-frequency shifts of 15 and 11 cm^{-1} from that of TCNQ (2227 cm^{-1}). This result indicates the occurrence of intermolecular CT between $\mathbf{I}_n$–3CNQ and TCNQ molecules and gives the degrees of CT; $-2\zeta_{\text{C≡N}} = -0.34$ for ($\mathbf{I}_1$–3CNQ)$_2$(TCNQ) and $-\zeta_{\text{C≡N}} = -0.25$ for ($\mathbf{I}_6$–3CNQ)(TCNQ). The smaller value of ($\mathbf{I}_6$–3CNQ)(TCNQ) than that of ($\mathbf{I}_1$–3CNQ)$_2$(TCNQ) corresponds to those estimated by the MO calculation and *BLR* (Tables 2 and 3). The difference in the estimated δ values between these methods would be caused by the perturbation of crystal packing to the $\nu_{\text{C≡N}}$ values.[38] The C≡N stretching modes of the 3CNQ moieties in the complexes have multiple peaks, which show low-frequency shifts of 3–8 cm^{-1} (Figure 3). Assuming that such modes of the 3CNQ molecules soften with increasing the degree of CT similarly to TCNQ CT complexes, the low frequency shifts indicate that the intermolecular CT interaction increases the degree of intramolecular CT of $\mathbf{I}_n$–3CNQ molecules. The complicated pattern in the ($\mathbf{I}_1$–3CNQ)$_2$(TCNQ) complex would originate from the existence of two kinds of $\mathbf{I}_1$–3CNQ molecules having different molecular conformations (Figures 1a and 1b).

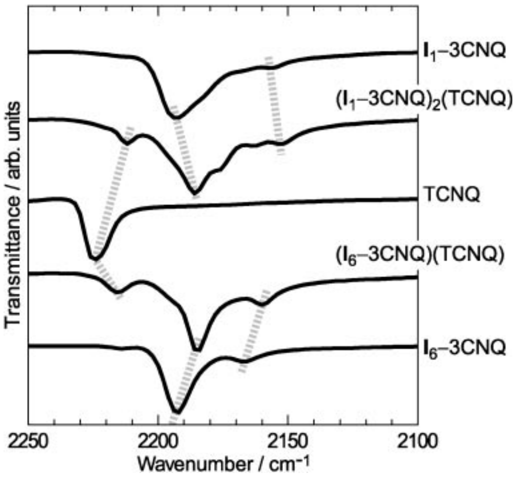

Figure 3. IR spectra (KBr pellet) of ($\mathbf{I}_1$–3CNQ)$_2$(TCNQ) and ($\mathbf{I}_6$–3CNQ)(TCNQ) with those of related compounds in the C≡N stretching region (2100–2250 cm^{-1}).

Table 5. C≡N Stretching Wavenumbers in the IR Spectra[a] and Intra- and Intermolecular CT Absorption Bands in the Solid-State[a] and Solution-State[b] (Bracket) UV–Vis–NIR Spectra of ($\mathbf{I}_1$–3CNQ)$_2$(TCNQ) and ($\mathbf{I}_6$–3CNQ)(TCNQ) and Related Compounds

	C≡N stretching modes/cm^{-1}		UV–vis–NIR spectra/nm	
	TCNQ	$\mathbf{I}_1$–3CNQ	Intermolecular CT	Intramolecular CT
($\mathbf{I}_1$–3CNQ)$_2$(TCNQ)	2212	2185, 2175, 2163, 2152	1156	858sh, 730 (786, 725)
$\mathbf{I}_1$–3CNQ		2193, 2156		865sh, 730 (787, 725)
($\mathbf{I}_6$–3CNQ)(TCNQ)	2216	2185, 2160	1132	842sh, 748 (806, 735)
$\mathbf{I}_6$–3CNQ		2190, 2163		844, 748 (805, 734)
TCNQ	2227			

a) Measured in KBr pellet. b) Measured in MeCN solution.

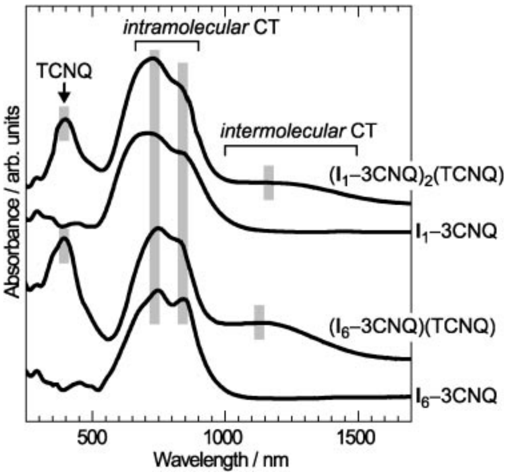

Figure 4. UV–vis–NIR spectra (KBr pellet) of ($\mathbf{I}_1$–3CNQ)$_2$(TCNQ) and ($\mathbf{I}_6$–3CNQ)(TCNQ) with those of related compounds.

Intra- and Intermolecular CT Absorption Bands in UV–Vis–NIR Spectra. The UV–vis–NIR spectra in an MeCN solution (see Supporting Information) of ($\mathbf{I}_1$–3CNQ)$_2$(TCNQ) and ($\mathbf{I}_6$–3CNQ)(TCNQ) are explained by simple superimpositions of those of neutral TCNQ and $\mathbf{I}_n$–3CNQ, where two major bands at around 400 and 500–900 nm, the latter of which has two major peaks, are observed. The former band is ascribable to the intramolecular excitation of neutral TCNQ, and the latter one originates from the intramolecular CT process of $\mathbf{I}_n$–3CNQ. Absorption bands originating from TCNQ radical anion species and intermolecular CT were not observed in the solution state.

Figure 4 shows the solid-state UV–vis–NIR spectra of the complexes, and Table 5 summarizes the CT transition bands in the solution and solid states. In the solid state, the intramolecular CT bands of both complexes as well as $\mathbf{I}_n$–3CNQ show red shifts from those in the solution state due to the highly polarized environment of bulk crystals (Table 5). The solid-state spectra exhibit additional broad absorption bands at 1000–1500 nm, which are ascribed to the intermolecular CT bands between 3CNQ and TCNQ, similar to those observed in CT complexes with alternating D···A stacks.[39] The peak energies of the CT absorption bands, 1156 nm (8.7×10^3 cm^{-1}) for ($\mathbf{I}_1$–3CNQ)$_2$(TCNQ) and 1132 nm (8.8×10^3 cm^{-1}) for ($\mathbf{I}_6$–3CNQ)(TCNQ), agree with the neutral ground state from the estimations of degrees of intermolecular CT. The intermolecular CT energies are higher than those of (BEDT-TTF)(TCNQ) complex in the neutral phase (5.7×10^3 cm^{-1})[36] and (DBTTF)(TCNQ) (7.4×10^3 cm^{-1}),[39] whose donor molecules have similar electron-donating abilities ($E_{1/2}{}^{\mathrm{ox}} = +0.53$ and $+0.62$ V vs. SCE, respectively) to those of $\mathbf{I}_n$–3CNQ.

Conclusion

Indoline–tricyanoquinodimethane type intramolecular CT compounds ($\mathbf{I}_n$–3CNQ, $n = 1$ and 6) gave CT complexes with TCNQ at 2:1 and 1:1 ratios, respectively. Structural analyses elucidated that $\mathbf{I}_n$–3CNQ molecules interact at the 3CNQ moieties with TCNQ through π-stacking interaction to establish one-dimensional columns. The estimations of degrees of intra- and intermolecular CT based on the MO calculation, bond lengths, and vibration spectra indicate that (1) the CT complexes between $\mathbf{I}_n$–3CNQ and TCNQ have neutral ground states, (2) intra- and intermolecular CT coexist in the CT complexes to give weakly ionized TCNQ molecules, and (3) intermolecular CT processes increase the degree of intramolecular CT of $\mathbf{I}_n$–3CNQ. Intermolecular CT processes in the complexes are evidenced by the solid-state UV–vis–NIR spectra, where low-energy absorptions assignable as intermolecular CT bands between $\mathbf{I}_n$–3CNQ and TCNQ are observed around 1000–1500 nm.

Both intramolecular CT compounds and CT complexes have been intensively studied in the development of molecule-based materials; however, they exhibit significantly different physical properties and functions. We emphasize that the present study shows not only the simple combination of two kinds of phenomena, but also will provide new strategies in the development of multifunctional organic materials. To make deeper discussion on the correlation between intra- and intermolecular CT processes and to discover novel functions of this kind of materials, the exploration of complexes having larger degrees of intermolecular CT by complex formation of $\mathbf{I}_n$–3CNQ-R with strong acceptor and donor molecules is indispensable. The next target of this kind of material is complexes with mixed-valent intermolecular CT states exhibiting high electrical conductivity, where the flexible electronic state and large dipole moment of the intramolecular CT compounds sensitive to the environmental perturbations, would control the degrees of intermolecular CT and their functions.

This work was partly supported by a Grant-in-Aid (21st Century COE programs on Kyoto University Alliance for Chemistry and No. 15205019) from the Ministry of Education, Culture, Sports, Science and Technology, Japan. T.M. is a recipient of a Japan Society for the Promotion of Science (JSPS) research fellowship.

Supporting Information

Dihedral angles of $\mathbf{I}_n$–3CNQ molecules, overlap mode in the crystal structures of $(\mathbf{I}_1\text{–3CNQ})_2$(TCNQ) and ($\mathbf{I}_6$–3CNQ)(TCNQ), UV–vis–NIR spectra in the solution state. This material is available free of charge at http://www.csj.jp/journals/bcsj/.

References

1 G. J. Ashwell, *Thin Solid Films* **1990**, *186*, 155.

2 A. M. R. Beaudin, N. Song, Y. Bai, L. Men, J. P. Gao, Z. Y. Wang, M. Szablewski, G. Cross, W. Wenseleers, J. Campo, E. Goovaerts, *Chem. Mater.* **2006**, *18*, 1079.

3 M. Szablewski, P. R. Thomas, A. Thornton, D. Bloor, G. H. Cross, J. M. Cole, J. A. K. Howard, M. Malagoli, F. Meyers, J.-L. Brédas, W. Wenseleers, E. Goovaerts, *J. Am. Chem. Soc.* **1997**, *119*, 3144.

4 a) S. R. Marder, C. B. Gorman, B. G. Tiemann, J. W. Perry, G. Bourhill, K. Mansour, *Science* **1993**, *261*, 186. b) S. R. Marder, C. B. Gorman, F. Meyers, J. W. Perry, G. Bourhill, J.-L. Brédas, B. M. Pierce, *Science* **1994**, *265*, 632. c) F. Meyers, S. R. Marder, B. M. Pierce, J. L. Brédas, *J. Am. Chem. Soc.* **1994**, *116*, 10703.

5 M. Barzoukas, C. Runser, A. Fort, M. Blanchard-Desce, *Chem. Phys. Lett.* **1996**, *257*, 531.

6 D. J. Williams, *Angew. Chem., Int. Ed. Engl.* **1984**, *23*, 690.

7 H. E. Katz, K. D. Singer, J. E. Sohn, C. W. Dirk, L. A. King, H. M. Gordon, *J. Am. Chem. Soc.* **1987**, *109*, 6561.

8 a) J. Garín, J. Orduna, J. I. Rupérez, R. Alcalá, B. Villacampa, C. Sánchez, N. Martín, J. L. Segura, M. González, *Tetrahedron Lett.* **1998**, *39*, 3577. b) M. R. Bryce, A. Green, A. J. Moore, D. F. Perepichka, A. S. Batsanov, J. A. K. Howard, I. Ledoux-Rak, M. González, N. Martín, J. L. Segura, J. Garín, J. Orduna, R. Alcalá, B. Villacampa, *Eur. J. Org. Chem.* **2001**, 1927.

9 S. Alías, R. Andreu, M. A. Cerdán, S. Franco, J. Garín, J. Orduna, P. Romero, B. Villacampa, *Tetrahedron Lett.* **2007**, *48*, 6539.

10 a) T. Kogej, D. Beljonne, F. Meyers, J. W. Perry, S. R. Marder, J. L. Brédas, *Chem. Phys. Lett.* **1998**, *298*, 1. b) D. Beljonne, T. Kogej, S. R. Marder, J. W. Perry, J. L. Brédas, *Mol. Cryst. Liq. Cryst. Sci. Technol., Sect. B* **1999**, *21*, 461.

11 J. C. May, I. Biaggio, F. Bures, F. Diederich, *Appl. Phys. Lett.* **2007**, *90*, 251106.

12 a) K. Higashino, T. Nakaya, E. Ishiguro, *J. Photochem. Photobiol., A* **1994**, *79*, 81. b) R. M. Williams, J. M. Zwier, J. W. Verhoeven, *J. Am. Chem. Soc.* **1995**, *117*, 4093. c) S. Kim, H. Choi, C. Baik, K. Song, S. O. Kang, J. Ko, *Tetrahedron* **2007**, *63*, 11436.

13 a) G. J. Ashwell, E. J. C. Dawnay, A. P. Kuczynski, M. Szablewski, I. M. Sandy, M. R. Bryce, A. M. Grainger, M. Hasan, *J. Chem. Soc., Faraday Trans.* **1990**, *86*, 1117. b) Y. Onganer, M. Yin, D. R. Bessire, E. L. Quitevis, *J. Phys. Chem.* **1993**, *97*, 2344.

14 Comprehensive reviews for unimolecular rectifiers based on $\mathrm{D}^{\delta+}$–π–$\mathrm{A}^{\delta-}$ molecules: a) R. M. Metzger, *Acc. Chem. Res.* **1999**, *32*, 950. b) R. M. Metzger, *J. Mater. Chem.* **1999**, *9*, 2027. c) R. M. Metzger, *Chem. Rev.* **2003**, *103*, 3803. d) R. M. Metzger, *Anal. Chim. Acta* **2006**, *568*, 146.

15 R. M. Metzger, N. E. Heimer, G. J. Ashwell, *Mol. Cryst. Liq. Cryst.* **1984**, *107*, 133.

16 R. M. Metzger, B. Chen, U. Höpfner, M. V. Lakshmikantham, D. Vuillaume, T. Kawai, X. Wu, H. Tachibana, T. V. Hughes, H. Sakurai, J. W. Baldwin, C. Hosch, M. P. Cava, L. Brehmer, G. J. Ashwell, *J. Am. Chem. Soc.* **1997**, *119*, 10455.

17 A. Honciuc, A. Otsuka, Y.-H. Wang, S. K. McElwee, S. A. Woski, G. Saito, R. M. Metzger, *J. Phys. Chem. B* **2006**, *110*, 15085.

18 G. J. Ashwell, W. D. Tyrrell, A. J. Whittam, *J. Am. Chem. Soc.* **2004**, *126*, 7102.

19 G. Wen, Y. Wang, Y. Song, Z. Lu, D. Zhang, Y. Liu, D. Zhu, *Chem. Phys. Lett.* **2006**, *431*, 370.

20 J. Ferraris, D. O. Cowan, V. Walatka, Jr., J. H. Perlstein, *J. Am. Chem. Soc.* **1973**, *95*, 948.

21 G. Saito, J. P. Ferraris, *Bull. Chem. Soc. Jpn.* **1980**, *53*, 2141.

22 J. B. Torrance, *Acc. Chem. Res.* **1979**, *12*, 79.

23 T. Ishiguro, K. Yamaji, G. Saito, *Organic Superconductors*, 2nd ed., Springer-Verlag, Berlin, **1998**.

24 G. Saito, T. Murata, *Philos. Trans. R. Soc. London, Ser. A* **2008**, *366*, 139.

25 J. S. Miller, A. J. Epstein, W. M. Reiff, *Chem. Rev.* **1988**, *88*, 201.

26 J. B. Torrance, J. E. Vazquez, J. J. Mayerle, V. Y. Lee, *Phys. Rev. Lett.* **1981**, *46*, 253.

27 S. Horiuchi, R. Kumai, Y. Okimoto, Y. Tokura, *Chem. Phys.* **2006**, *325*, 78.

28 M. Chollet, L. Guerin, N. Uchida, S. Fukaya, H. Shimoda, T. Ishikawa, K. Matsuda, T. Hasegawa, A. Ota, H. Yamochi, G. Saito, R. Tazaki, S. Adachi, S. Koshihara, *Science* **2005**, *307*, 86.

29 Several CT complexes of D–σ–A compounds have been reported, see: a) N. Martín, L. Sánchez, C. Seoane, R. Andreu, J. Garín, J. Orduna, *Tetrahedron Lett.* **1996**, *37*, 5979. b) N. Martín, L. Sánchez, C. Seoane, R. Andreu, J. Garín, J. Orduna, E. Ortí, P. M. Viruela, R. Viruela, *J. Phys. Chem. Solids* **1997**, *58*, 1713.

30 G. Saito, C.-H. Chong, M. Makihara, A. Otsuka, H. Yamochi, *J. Am. Chem. Soc.* **2003**, *125*, 1134.

31 T. Murata, K. Nishimura, Y. Enomoto, G. Honda, Y. Shimizu, A. Otsuka, G. Saito, *Bull. Chem. Soc. Jpn.* **2008**, *81*, 869.

32 T. Murata, G. Saito, K. Nishimura, C.-H. Chong, M. Makihara, G. Honda, Y. Enomoto, S. Khasanov, H. Yamochi, A. Otsuka, K. Kamada, K. Ohta, J. Kawamata, *Bull. Chem. Soc. Jpn.* **2008**, *81*, 1131.

33 G. M. Sheldrick, *Program for the Solution of Crystal Structuers*, University of Göttingen, Göttingen, Germany, **1997**.

34 G. M. Sheldrick, *Program for the Refinement of Crystal Structures*, University of Göttingen, Göttingen, Germany, **1997**.

35 H. Kobayashi, J. Nakayama, *Bull. Chem. Soc. Jpn.* **1981**, *54*, 2408.

36 G. Saito, H. Hayashi, T. Enoki, H. Inokuchi, *Mol. Cryst.*

Liq. Cryst. **1985**, *120*, 341.

37 a) S. Flandrois, D. Chasseau, *Acta Crystallogr., Sect. B* **1977**, *33*, 2744. b) T. J. Kistenmacher, T. J. Emge, A. N. Bloch, D. O. Cowan, *Acta Crystallogr., Sect. B* **1982**, *38*, 1193.

38 J. S. Chappell, A. N. Bloch, W. A. Bryden, M. Maxfield, T. O. Poehler, D. O. Cowan, *J. Am. Chem. Soc.* **1981**, *103*, 2442. It should be noted that the authors of this paper used both b_{1u} and a_g modes of C≡N stretching in their analysis. If one uses only b_{1u} modes of IR spectra, the linear relation between $\nu_{C\equiv N}$ and the degree of CT is held only below 0.5.

39 J. B. Torrance, B. A. Scott, B. Welber, F. B. Kaufman, P. E. Seiden, *Phys. Rev. B* **1979**, *19*, 730.